SECTION 4
REGRESSSION ANALYSIS OF THE SEMI-EMPRICAL MODELS

The regression analyses of the semi-empirical models of Eqs.(2.21) through (2.23) were carried out by using the data in Table A-1 with the help of the least-square technique. As mentioned previously, our regression analyses consist of two phases. In the first phase the appropriate values of $\mathbf{r_t}$ are determined using the acceleration model. In the second phase the velocity and displacement models are established using the results for $\mathbf{r_t}$ from the acceleration model. In addition, we need to assign a reference site whose dummy variable $\mathbf{S_j}$ is not given and virtually set to be zero in Eqs.(2.21) through (2.23). Such a reference site, of course, can be picked arbitrarily from any of the observation sites. However our previous studies reveal that it is most desirable to assign a site where there exists outcrop hard enough to satisfy the condition of the seismic bed rock for the other sites. Although the selection of the seismic bed rock might vary according to the dominant frequency content, we initially selected the same reference site for acceleration, velocity and displacement motions on the condition that the definition of the seismic bed rock should be examined based on the resulting amplification factors at each observation site. Herein we choose OFUNATO labelled 12 in Fig. 3-1 as the reference site in accordance with the discussion in Kamiyama and Yanagisawa[9]. The OFUNATO site is situated at a rock outcrop having shear wave velocity in the 1 to 2 km/sec range.

4.1 Regression Analysis for the Acceleration Model

Table 4-I shows the summary of the regression coefficients analyzed for trial values of $\mathbf{r_c}$ in the acceleration model. In Table 4-I, the results of regression coefficients $\mathbf{A_1}$, $\mathbf{A_2}$,---, $\mathbf{A_{N-1}}$ are omitted because the main purpose of the table is to determine the most appropriate values for $\mathbf{b_1}$ and $\mathbf{b_2}$ based on the variations of $\mathbf{r_t}$ in terms of earthquake magnitude. For this reason, the variations of $\mathbf{r_t}$ estimated by Eq.(2.15) are indicated in Table 4-I in stead of the results of $\mathbf{A_i}$. Note that the multiple correlation coefficient **R**, which means the goodness of fit, is largest for $\mathbf{r_c}$ <10 km. Table 4-I also shows that the variation of $\mathbf{r_t}$ depends on $\mathbf{r_c}$ but it becomes relatively stable for $\mathbf{r_c \leq 5.3}$ km. As stated in the preceding section, $\mathbf{r_t}$ is closely related to a characteristic length of the earthquake fault. Hence in addition to the goodness of fit and stability of the $\mathbf{r_t}$ parameter, the choice of $\mathbf{b_1}$ and $\mathbf{b_2}$ is also based on the consistency of $\mathbf{r_t}$ with empirical estimates of fault length. Although the value of $\mathbf{r_t}$ is somewhat arbitrarily related to fault length, it is reasonable to interpret $\mathbf{r_t}$ as nearly equivalent to the radius of the fault which is assumed herein to be circular. The fault area of earthquake has been investigated by many workers. Typically it is related to earthquake magnitude. For instance, Sato[23] derived the following expression.

Table 4-I Regression Coefficients, Multiple Correlation Coefficient, Standard Deviation and r_t for Acceleration Model

	r_c (km)															
	50	40	30	20	10	8.0	6.0	5.8	5.6	5.4	5.3	5.2	5.1	4.8	4.6	4.4
b_1	-1.766	-1.760	-1.555	-1.266	-0.767	-0.608	-0.403	-0.379	-0.354	-0.819	-1.164	-1.150	-1.137	-1.093	-1.063	-1.031
b_2	0.324	0.333	0.333	0.333	0.332	0.332	0.332	0.332	0.332	0.345	0.358	0.358	0.358	0.358	0.358	0.358
c_a	2.126	2.228	2.228	2.228	2.228	2.228	2.283	2.228	2.228	2.637	2.910	2.910	2.910	2.910	2.910	2.910
R	0.845	0.854	0.862	0.876	0.896	0.900	0.905	0.906	0.906	0.894	0.890	0.890	0.890	0.891	0.891	0.891
S	0.228	0.227	0.227	0.227	0.228	0.228	0.228	0.228	0.228	0.243	0.247	0.247	0.247	0.247	0.247	0.247
r_t (km) M=5	41.3	35.1	35.1	35.1	35.1	35.1	35.1	35.1	35.1	19.3	12.8	12.8	12.8	12.8	12.8	12.8
M=6	65.1	56.0	56.0	56.0	56.0	56.0	56.0	56.0	56.0	31.3	21.2	21.2	21.2	21.2	21.2	21.2
M=7	102.6	89.4	89.4	89.4	89.3	89.3	89.3	89.3	89.3	50.8	35.0	34.9	34.9	35.0	35.0	35.0
M=8	161.7	142.8	142.8	142.8	142.5	142.5	142.5	142.5	142.5	82.5	57.9	57.8	57.8	57.9	57.9	57.9

b_1, b_2 and c_a=regression coefficients , M= earthquake magnitude
R=multiple correlation coefficient
S= standard deviation

$$r_t = r_c \times 10^{\frac{b_1 + b_2 M}{1.64}}$$

$$S = 10^{M-4.07} \tag{4.1}$$

where S is the area of the fault in square kilometers.

Table 4-II shows the variation of fault radius obtained from Eq.(4.1) assuming a circular fault. A comparison between Table 4-I and Table 4-II indicates that values of $\mathbf{r_c}$ less than or equal to **5.3** km yield the best match between $\mathbf{r_t}$ and empirical estimates of the fault radius by others, even though there is some difference between them. The difference may be due to the possibility that $\mathbf{r_t}$ is related to a characteristic length of a rectangular fault rather than the radius of circular fault. Accordingly, we choose $\mathbf{b_1 = -1.164}$, $\mathbf{b_2 = 0.358}$ and $\mathbf{c_a = 2.91}$, which were obtained by setting $\mathbf{r_c = 5.3}$ km, for the acceleration model of Eq.(2.21). The regression coefficients $\mathbf{A_1}$, $\mathbf{A_2}$, ---, $\mathbf{A_{N-1}}$ in Eq.(2.21), which were obtained based on $\mathbf{r_c = 5.3}$, are shown in Table 4-III. In Table 4-III, $\mathbf{A_i}$ **(i=1~N-1)** are given for each observation site except the reference site. Hence the eventual semi-empirical expression for the peak horizontal ground acceleration is

$$a_{max}(i,M,r) = 10^{2.910} 10^{A_i} \qquad (r \le 10^{0.014+0.218M}) \tag{4.2}$$

$$a_{max}(i,M,r) = 10^{2.933+0.358M-1.64\log_{10} r} \times 10^{A_i} \qquad (r > 10^{0.014+0.218M}) \tag{4.3}$$

where $\mathbf{A_i}$ are given in Table 4-III on the condition that $\mathbf{A_i = 0}$ for the reference site.

4.2 Regression Analysis for the Velocity and Displacement Models

The regression coefficients of the velocity and displacement models of Eqs.(2.22) and (2.23) are presented in Table 4-IV, based on $\mathbf{b_1 = -1.164}$ and $\mathbf{b_2 = 0.358}$ from the acceleration model. Hence the semi-empirical expressions for the peak horizontal ground velocity and displacement are

$$v_{max}(i,M,r) = 10^{0.535+0.153M} \times 10^{B_i} \qquad (r \le 10^{0.014+0.218M}) \tag{4.4}$$

$$v_{max}(i,M,r) = 10^{0.558+0.511M-1.64\log_{10} r} \times 10^{B_i} \qquad (r > 10^{0.014+0.218M}) \tag{4.5}$$

$$d_{max}(i,M,r) = 10^{-0.522+0.236M} \times 10^{D_i} \qquad (r \le 10^{0.014+0.218M}) \tag{4.6}$$

Table 4-II Fault Radius Based on the Sato[23] Relation for Fault Area

MAGNITUDE M	RADIUS (KM)
5	1.65
6	5.21
7	16.46
8	52.05

Table 4-III Site Amplification Coefficients for Acceleration Model

NO	SITE NAME	A_i
1	KUSHIRO	0.196
2	CHIYODA	0.127
3	TOKACHI	0.110
4	HOROMAN	-0.202
5	SHIN ISHIKARI	0.396
6	TOMAKOMAI	0.129
7	MURORAN	0.271
8	AOMORI	0.090
9	HACHINOHE	-0.098
10	MAZAKI	-0.092
11	MIYAKO	0.194
12	OFUNATO	---.-----
13	SHIOGAMA	0.193
14	TAIRA	0.046
15	SHINTONE	-0.092
16	KASHIMA JIMU	-0.002
17	KASHIMA PWR	-0.047
18	TONE ESD	-0.139
19	OMIGAWA	-0.104
20	CHIBA	0.021
21	YAMASHITA HEN	-0.123
22	KANNONZAKI	0.129
23	OCHIAI C	-0.768
24	KINOKAWA	-0.771
25	ITAJIMA	0.349
26	HOSOSHIMA	-0.113
27	SOMA	0.239
28	SHINAGAWA	0.032
29	ONAHAMA JI	0.076
30	AKITA	-0.037
31	CHIBA S	-0.032
32	HITACHI NAKA	0.135
33	KASHIMA ZOKAN	0.016

Table 4-IV Regression Coefficients, Site Amplification Coefficients, Multiple Coefficient and Standard Deviation for Velocity and Displacement models

REGRESSION COEFFICIENTS		MAX. VEL	MAX. DIS
α, δ		0.153	0.236
b_1		-1.164	-1.164
b_2		0.358	0.358
c_v , c_d		0.535	-0.522
B_i ,D_i			
1	KUSHIRO	0.431	0.345
2	CHIYODA	0.296	0.294
3	TOKACHI	0.127	0.151
4	HOROMAN	-0.295	-0.302
5	SHIN ISHIKARI	0.748	0.662
6	TOMAKOMAI	0.255	0.241
7	MURORAN	0.313	0.213
8	AOMORI	0.488	0.494
9	HACHINOHE	0.131	0.176
10	MAZAKI	0.039	0.409
11	MIYAKO	0.033	-0.034
12	OFUNATO	--.-----	--.-----
13	SHIOGAMA	0.465	0.161
14	TAIRA	0.310	0.282
15	SHINTONE	0.298	0.204
16	KASHIMA JIMU	0.364	0.239
17	KASHIMA PWR	0.294	0.089
18	TONE ESD	0.346	0.568
19	OMIGAWA	0.357	0.587
20	CHIBA	0.314	0.432
21	YAMASHITA HEN	0.116	0.051
22	KANNONZAKI	0.179	0.067
23	OCHIAI C	-0.534	-0.641
24	KINOKAWA	-0.568	-0.650
25	ITAJIMA	0.356	0.207
26	HOSOSHIMA	0.051	-0.118
27	SOMA	0.110	-0.088
28	SHINAGAWA	0.358	0.136
29	ONAHAMA JI	0.112	0.099
30	AKITA	0.227	0.248
31	CHIBA S	0.342	0.176
32	HITACHI NAKA	0.053	-0.496
33	KASHIMA ZOKAN	0.133	0.050
MULTIPLE CORRELATION COEFFICI.		0.770	0.848
STANDARD DEVIATION		0.264	0.272

$$d_{max}(i,M,r) = 10^{-0.499 + 0.594\ M - 1.64 \log_{10} r} \times 10^{D_i} \qquad (r > 10^{0.014 + 0.218 M}) \tag{4.7}$$

where $\mathbf{B_i}$ and $\mathbf{D_i}$ are given in Table 4-4 on the condition that $\mathbf{B_i = 0}$ or $\mathbf{D_i = 0}$ for the reference site.

Finally, adequacy of the semi-empirical model was checked statistically by inspection of the residuals plots. The residual, which is simply the ratio of the observed to predicted velocities from Eqs.(4.4) and (4.5), were plotted as functions of each independent variable. The residual plots for peak velocity are illustrated in Figs. 4-1 through 4-3. The fact that no particular trend was observed in the residual plots implies that the proposed semi-empirical model is adequate from a statistical point of view.

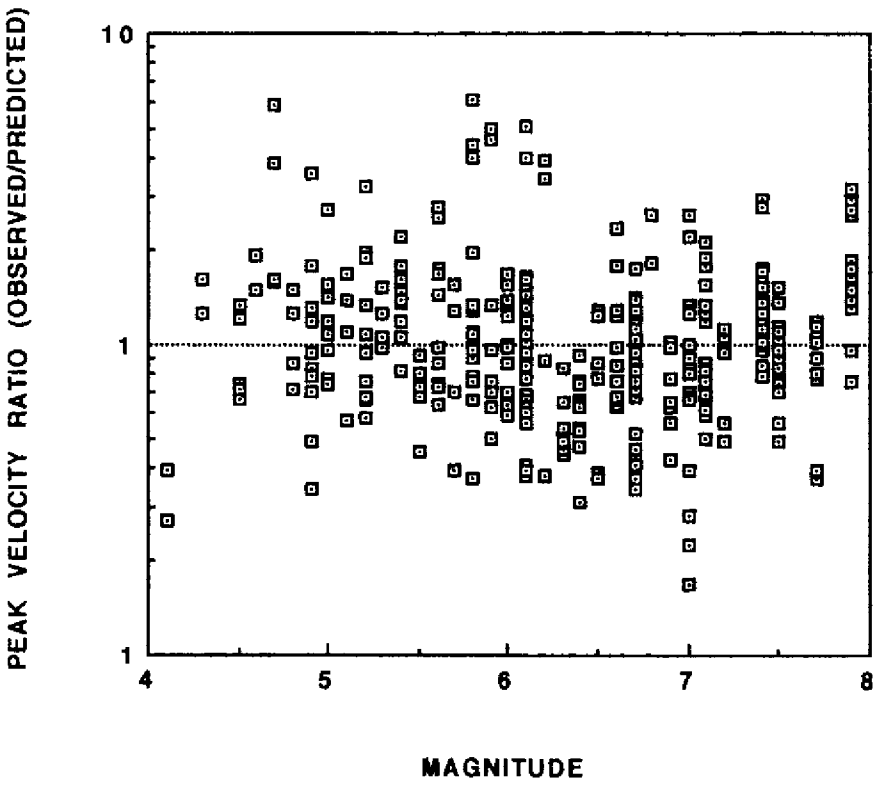

Fig.4-1 Residual Plots of Peak Velocity versus Magnitude

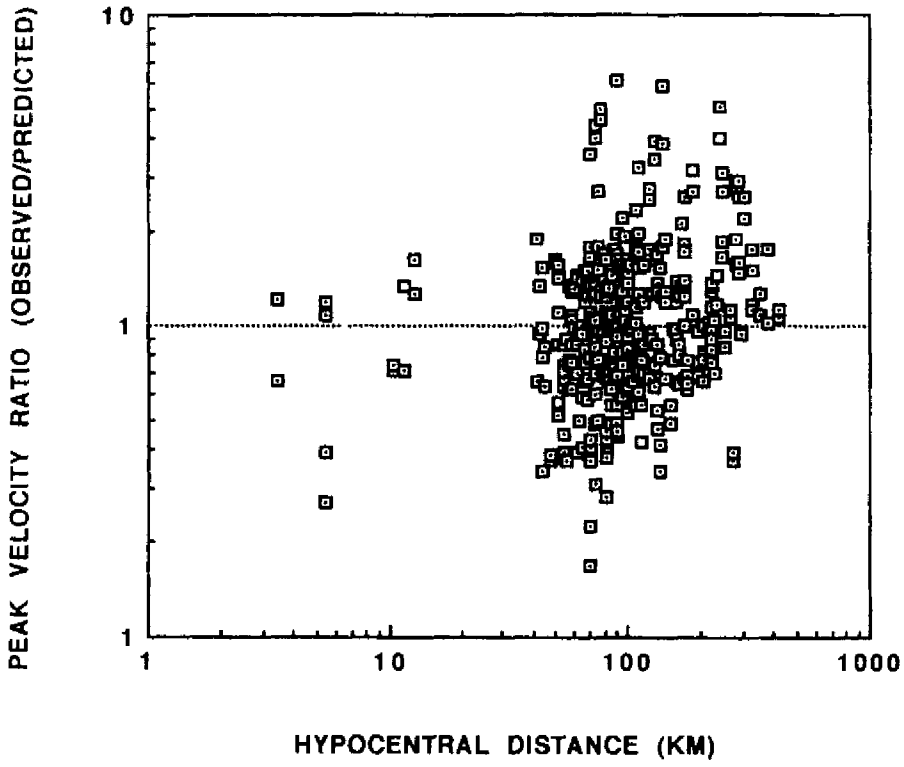

Fig.4-2 Residual Plots of Peak Velocity versus Hypocentral Distance

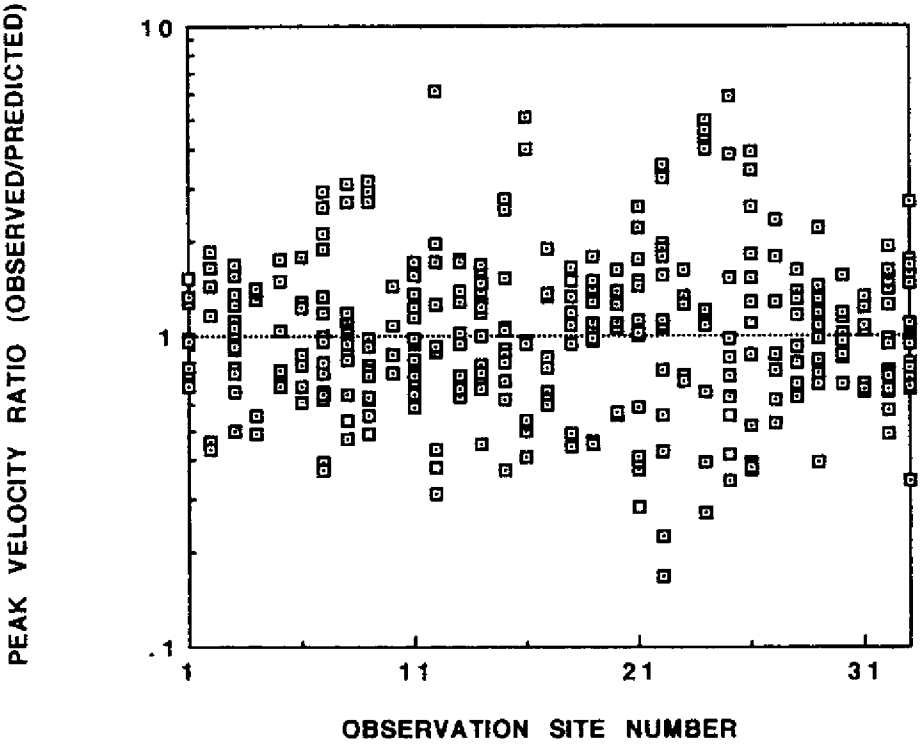

Fig.4-3 Residual Plots of Peak Velocity versus Observation Site Number

SECTION 5
AMPLIFICATION DUE TO LOCAL SITE CONDITIONS

The proposed semi-empirical model provides local soil amplification factors for the peak values at each site. In this section, the amplification factors are discussed in terms of the soil conditions at the sites as well as the frequency content of the motions.

5.1 Amplification Factors for the Peak Acceleration, Velocity and Displacement

As implied in Eq.(4.2) to Eq.(4.7), the amplification factor at each site is given by 10^{A_i}, 10^{B_i} or 10^{D_i} with respect to the reference site which was selected as a candidate to satisfy the condition of the seismic bed rock. Table 5-I lists the amplification factors obtained for the peak acceleration, velocity and displacement at each site along with their mean values and standard deviations. In Table 5-I, the amplification factor at the reference site (OFUNATO) is set to be one by definition. We can see from Table 5-I that the amplification factors vary markedly from site to site probably reflecting the difference in the soil conditions. In addition, the variations of the amplification factors differ depending on the type of motion characteristics: acceleration, velocity and displacement. This significant variation in amplification factors indicates the importance of taking individual site conditions into consideration, as contrasted with the rough classification schemes of soil conditions employed in the past studies. The averages and standard deviations in Table 5-I also reveal that the peak acceleration is less dependent on local site conditions than the peak velocity and displacement. Correlations between the amplification factors for the peak acceleration, velocity and displacement are shown in Figs.5-1 to 5-3. Note that, as shown in Figs.5-1 and 5-2, the amplification factor for peak acceleration is not well correlated with the amplification factors for peak velocity and peak displacement, while Fig.5-3 shows that the amplification factor for peak velocity is fairly well correlated with that for peak displacement. This suggests that there is a difference in the mechanism and frequency content between acceleration motion and the other motions such as velocity and displacement when they are amplified through surface soils.

It is noted in Table 5-I that the two observation sites, OCHIAI C and KINOKAWA give very small amplification factors for the peak acceleration, peak velocity and peak displacement. These amplification factors are considerably smaller than that for the reference site(OFUNATO). The recording conditions of strong motions at these two sites are the most likely reason. Note that almost all the strong-motion records observed at the two sites are lacking in a part of the main-

Table 5-I Amplification Factors for Peak Acceleration, Peak Velocity and Peak Displacement

		AMPLIFICATION FACTORS		
NO	SITE NAME	ACC	VEL	DIS
1	KUSHIRO	1.57	2.70	2.21
2	CHIYODA	1.30	1.98	1.97
3	TOKACHI	1.29	1.34	1.42
4	HOROMAN	0.63	0.51	0.50
5	SHIN ISHIKARI	2.49	5.59	4.67
6	TOMAKOMAI	1.35	1.80	1.74
7	MURORAN	1.86	2.05	1.63
8	AOMORI	1 23	3.08	3.12
9	HACHINOHE	0.80	1.35	1.50
10	MAZAKI	0.81	1.09	2.56
11	MIYAKO	1.56	1.08	0.92
12	OFUNATO	1.00	1.00	1.00
13	SHIOGAMA	1.56	2.91	1.45
14	TAIRA	1.11	2.04	1.91
15	SHINTONE	0.81	1.99	1.60
16	KASHIMA JIMU	1.00	2.31	1.73
17	KASHIMA PWR	0.89	1.97	1.23
18	TONE ESD	0.73	2.27	3.70
19	OMIGAWA	0.79	2.27	3.86
20	CHIBA	1.05	2.06	2.70
21	YAMASHITA HEN	0.76	1.45	1.12
22	KANNONZAKI	1.35	1.51	1.17
23	OCHIAI C	0.17	0.29	0.23
24	KINOKAWA	0.17	0.28	0.22
25	ITAJIMA	2.23	2.27	1.61
26	HOSOSHIMA	0.74	1.12	0.76
27	SOMA	1.73	1.29	0.82
28	SHINAGAWA	1.08	2.28	1.37
29	ONAHAMA JI	1.19	1.31	1.26
30	AKITA	0.92	1.68	1.77
31	CHIBA S	0.93	2.20	1.50
32	HITACHI NAKA	1.36	1.13	0.32
33	KASHIMA ZOKAN	1.03	1.36	1.12
	AVERAGE	1.136	1.805	1.657
	SD	0.497	0.965	1.027

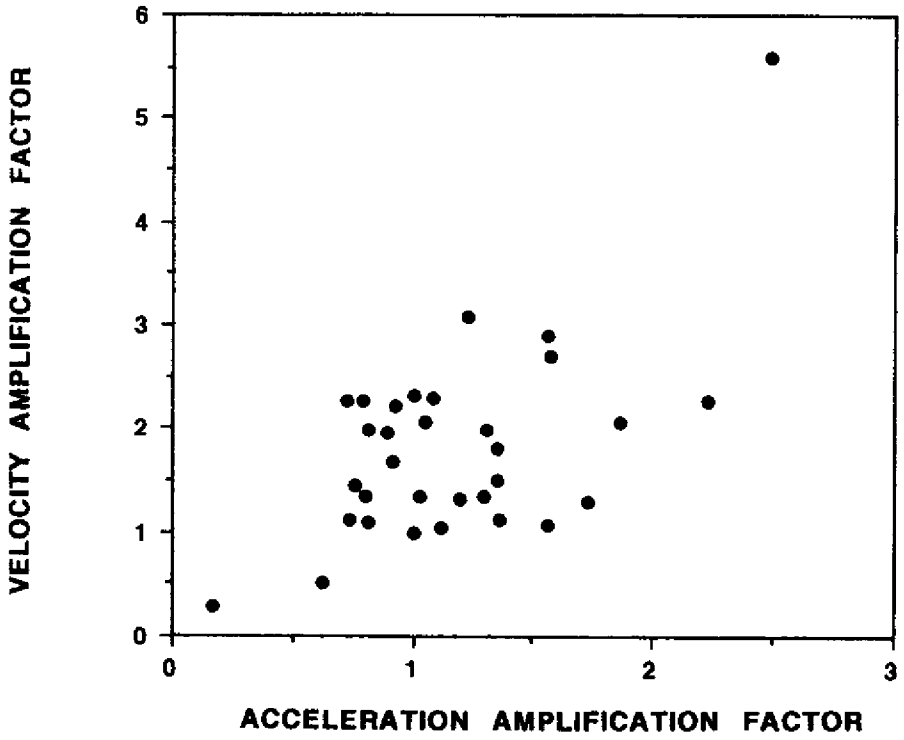

Fig.5-1 **Scattergram of Velocity and Acceleration Amplification Factors (Correlation Coefficient =0.635)**

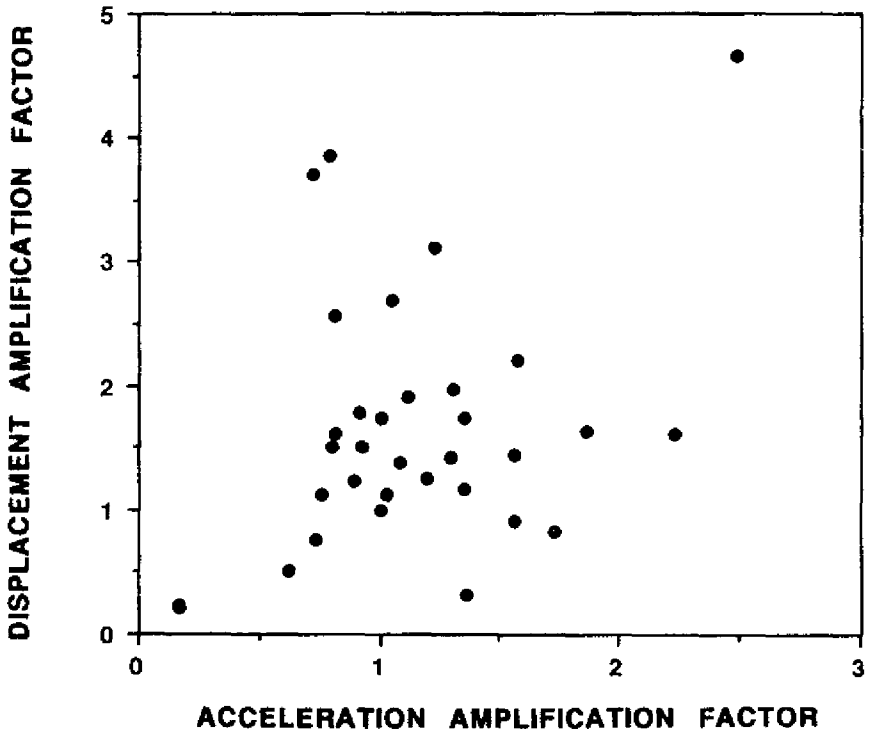

Fig.5-2 Scattergram of Displacement and Acceleration Amplification Factors (Correlation Coefficient=0.329)

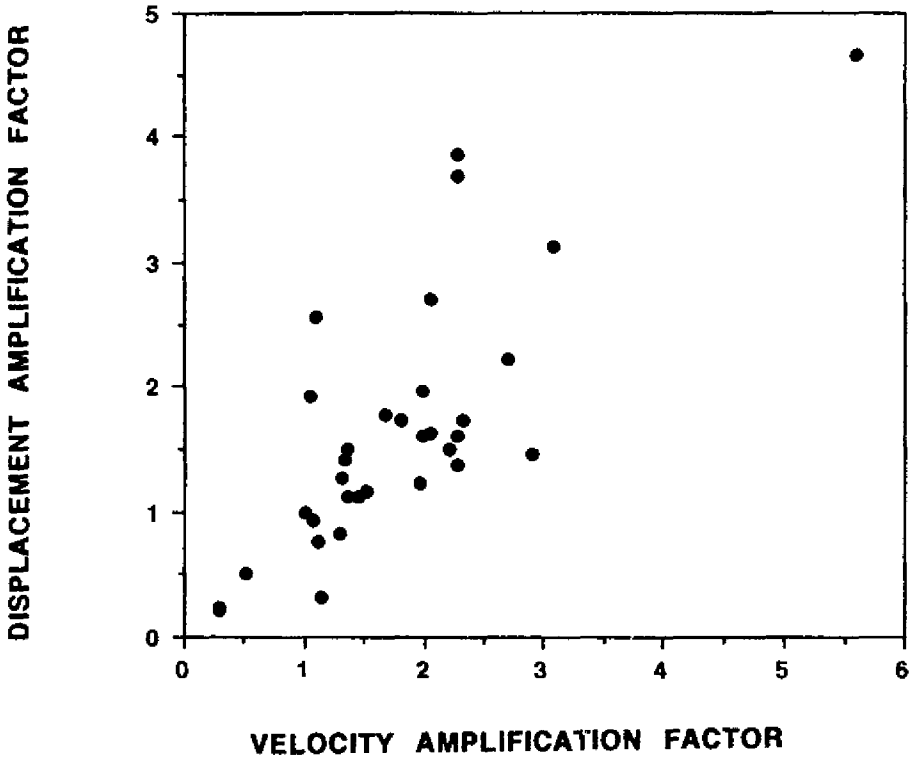

Fig.5-3 Scattergram of Displacement and Velocity Amplification Factors (Correlation Coefficient=0.767)

motions as well as first-motions, resulting from miss triggering of the recording instruments. Incompleteness of the recordings is considered to affect the peak values of acceleration, velocity and displacement at both sites because they were obtained through band-pass filtering as well as the instrument correction. Hence the two sites of OCHIAI C and KINOKAWA are exempted from the discussion of amplification in terms of frequency and local soils which will be described in a later section.

The same reference site was selected for all three motions; acceleration, velocity and displacement. At the same time, OFUNATO was assigned to the reference site as a candidate satisfying the condition of the seismic bed rock for the other sites. However, the difference in the variations of amplification factors for the three motions indicates that the reference site should be selected differently depending on the motion characteristics. In fact, the absolute values of the amplification factors in Table 5-I differ for the peak acceleration, velocity and displacement. Note that, for example, the average amplification factor for the peak acceleration is only slightly larger than 1.0 which is the amplification factor for the reference site, whereas the average amplification factors for the peak velocity and displacement are roughly 1.8 and 1.7 respectively. Since local soil conditions generally amplify the motions incident to the seismic bed rock, the amplification factor is expected to be greater than 1.0 when the reference site is properly selected to satisfy the condition of the seismic bed rock. In the cases of the peak velocity and displacement in Table 5-I, the amplification factors at each site are almost always greater than 1.0, implying a relatively proper selection as seismic bed rock site. The amplification factors for the peak acceleration, on the other hand, show many values less than 1.0. This means that the reference site is improperly selected to satisfy the condition of seismic bed rock for the peak acceleration.

A possible way for obtaining more proper amplification factors is to redo the regression analysis for the peak acceleration by selecting another reference site. However this requires iteration because the selection of the reference site is not the only parameter controlling the amplification factors. Considering that we have obtained meaningful amplification factors as relative values even though they are controversial in the absolute values, we herein renovate the amplification factors in Table 5-I so as to meet the proper condition of amplification. That is, the amplification factors in Table 5-I are multiplied by a value to correspond to the definition of amplification factor with respect to the seismic bed rock. Though the inverse of the least amplification factor in each motion peak in Table 5-I can be a candidate for the multiplier, such simple multiplication gives little reasonable amplification factor because the least amplification factor involves more statistical errors. Herein we make an alternative attempt by renovating the amplification factors in Table 5-I so that the average value minus the one standard error is 1.0. For example, **1/(1.136-0.497)** is

multiplied to the amplification factors in the case of the peak acceleration. This is an attempt to make the amplification factors approach proper values with respect to the seismic bed rock while avoiding the statistical errors. The amplification factors for the peak velocity and peak displacement were also renovated in a similar manner. The final amplification factors for each motion peak are listed in Table 5-II. Note in Table 5-II that the definition of the seismic bed rock differs for peak acceleration, velocity and displacement as a result of the renovations. For example, HOROMAN, OFUNATO and HOROMAN correspond to the seismic bed rock site for the peak acceleration, velocity and displacement respectively because their renovated amplification factors are nearly equal to 1.0. A geological survey shows a rock outcrop at the HOROMAN site as well as OFUNATO. Table 5-II shows that the absolute values for the renovated amplification factors are always greater than 1.0 except at a few sites including OCHIAI C and KINOKAWA. Table 5-II also indicates that the average values of the renovated amplification factors increase proportionally from acceleration to displacement. This is consistent with a theoretical explanation from amplification phenomena through surface soils. That is, the amplification factor for velocity motion is theoretically expected to be greater than that for acceleration motion because velocity motion is generally affected by deeper soil layers with its dominant amplitude components in longer periods than acceleration motion. Similarly the amplification for displacement motion is greater than that for velocity motion.

As a result of the renovations for the amplification factors, the overall semi-empirical expressions of Eqs.(4.2) to (4.7) are modified so that the motion peaks on the seismic bed rock are diminished to offset the increased amplification factors resulting from the renovations. Denoting the renovated amplification factors at the i-th site in Table 5-II as $\mathbf{AMP_i(a)}$, $\mathbf{AMP_i(v)}$ and $\mathbf{AMP_i(d)}$ for the peak acceleration, peak velocity and peak displacement respectively, we rewrite the final semi-empirical expressions as follows:

(peak acceleration)

$$a_{max}(i,M,r) = (1.136 - 0.497) \times 10^{2.910} \times AMP_i(a) \qquad (r \le 10^{0.014+0.218M})$$

$$= 518.9 \times AMP_i(a) \qquad (r \le 10^{0.014+0.218M}) \qquad (5.1)$$

$$a_{max}(i,M,r) = 547.6 \times 10^{0.358M - 1.64\log_{10} r} \times AMP_i(a) \qquad (r > 10^{0.014+0.218M}) \qquad (5.2)$$

Table 5-II Renovated Amplification Factors for Peak Acceleration, Peak Velocity and Peak Displacement

		RENOVATED AMPLIFICATION FACTORS		
NO	SITE NAME	ACC	VEL	DIS
1	KUSHIRO	2.46	3 21	3.51
2	CHIYODA	2.03	2.36	3.13
3	TOKACHI	2.02	1.60	2.25
4	HOROMAN	0.99	0.61	0.79
5	SHIN ISHIKARI	3.90	6.66	7.41
6	TOMAKOMAI	2.11	2.14	2.76
7	MURORAN	2.91	2.44	2.59
8	AOMORI	1.92	3.67	4.95
9	HACHINOHE	1.25	1.61	2.38
10	MAZAKI	1.27	1.30	4.06
11	MIYAKO	2.44	1.29	1.46
12	OFUNATO	1.56	1.19	1.59
13	SHIOGAMA	2.44	3.46	2.30
14	TAIRA	1.74	2.43	3.03
15	SHINTONE	1.27	2.37	2.54
16	KASHIMA JIMU	1.56	2.75	2.75
17	KASHIMA PWR	1.39	2.35	1.95
18	TONE ESD	1.14	2.70	5.87
19	OMIGAWA	1.24	2.70	6.13
20	CHIBA	1.64	2.45	4.29
21	YAMASHITA HEN	1.19	1.73	1.78
22	KANNONZAKI	2.11	1.80	1.86
23	OCHIAI C	0.27	0.35	0.37
24	KINOKAWA	0.27	0.33	0.35
25	ITAJIMA	3.49	2.70	2.56
26	HOSOSHIMA	1.16	1.33	1.21
27	SOMA	2.71	1.54	1.30
28	SHINAGAWA	1.69	2.71	2.17
29	ONAHAMA JI	1.86	1.56	2.00
30	AKITA	1.44	2.00	2.81
31	CHIBA S	1.46	2.62	2.38
32	HITACHI NAKA	2.13	1.35	0.51
33	KASHIMA ZOKAN	1.61	1.62	1.78
	AVERAGE	1.778	2.149	2.630
	SD	0.778	1.149	1.630

(peak velocity)

$$v_{max}(i,M,r) = (1.805 - 0.965) \times 10^{0.535+0.153M} \times AMP_i(v) \quad (r \le 10^{0.014+0.218M})$$

$$= 2.879 \times 10^{0.153M} \times AMP_i(v) \quad (r \le 10^{0.014+0.218M}) \qquad (5.3)$$

$$v_{max}(i,M,r) = 3.036 \times 10^{0.511M - 1.64\log_{10} r} \times AMP_i(v) \quad (r > 10^{0.014+0.218M}) \qquad (5.4)$$

(peak displacement)

$$d_{max}(i,M,r) = (1.657 - 1.027) \times 10^{-0.522+0.236M} \times AMP_i(d) \quad (r \le 10^{0.014+0.218M})$$

$$= 0.189 \times 10^{0.236M} \times AMP_i(d) \quad (r \le 10^{0.014+0.218M}) \qquad (5.5)$$

$$d_{max}(i,M,r) = 0.200 \times 10^{0.594M - 1.64\log_{10} r} \times AMP_i(d) \quad (r > 10^{0.014+0.218M}) \qquad (5.6)$$

where $\mathbf{a_{max}}$ is peak acceleration(cm/sec^2), $\mathbf{v_{max}}$ is peak velocity(cm/sec), $\mathbf{d_{max}}$ is peak displacement(cm), **i** is the number for identifying the observation site, **M** is the earthquake magnitude, and **r** is the hypocentral distance(km).

5.2 Relation Between the Amplification Factors and Frequency Content

The above discussion reveals that local site effects for peak acceleration are different than those for peak velocity and displacement. This suggests that the dominant frequency component in acceleration, velocity and displacement motions plays a significant role in determining the amplification factor for peak values. In relation to the frequency content in strong motions, Kamiyama and Yanagisawa[9] derived amplification factors for response spectra using almost same strong-motion records and observation sites as in the present study. These spectral amplifications were presented in a frequency-dependent form. Hence they allow us to examine the frequency effect on the amplification factors for the peak values. Figs.5-4 to 5-8 show spectral amplification factors obtained by Kamiyama and Yanagisawa[9] at sites used in this study. No simple relation exists between the peak value and the spectral characteristics of ground motions

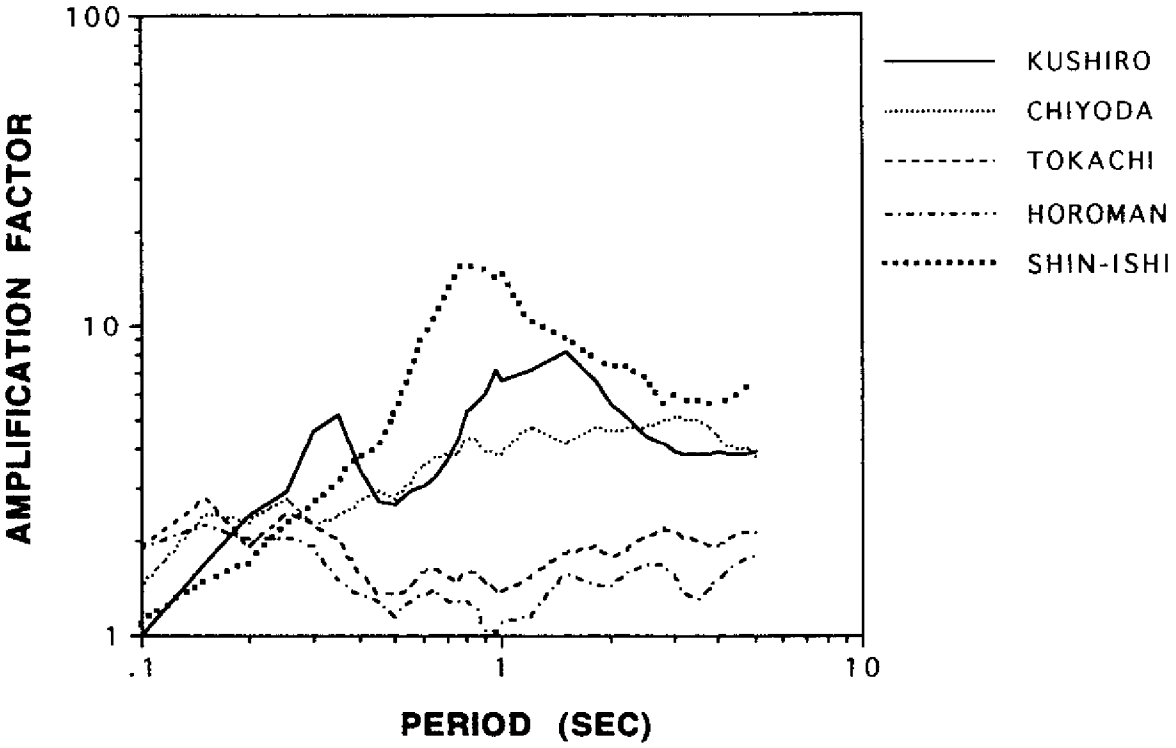

Fig.5-4 Response Spectra Amplification Factors for 5 Sites(Kushiro, Chiyoda, Tokachi, Horoman and Shin Ishikari) in Japan (after Kamiyama and Yanagisawa[9])

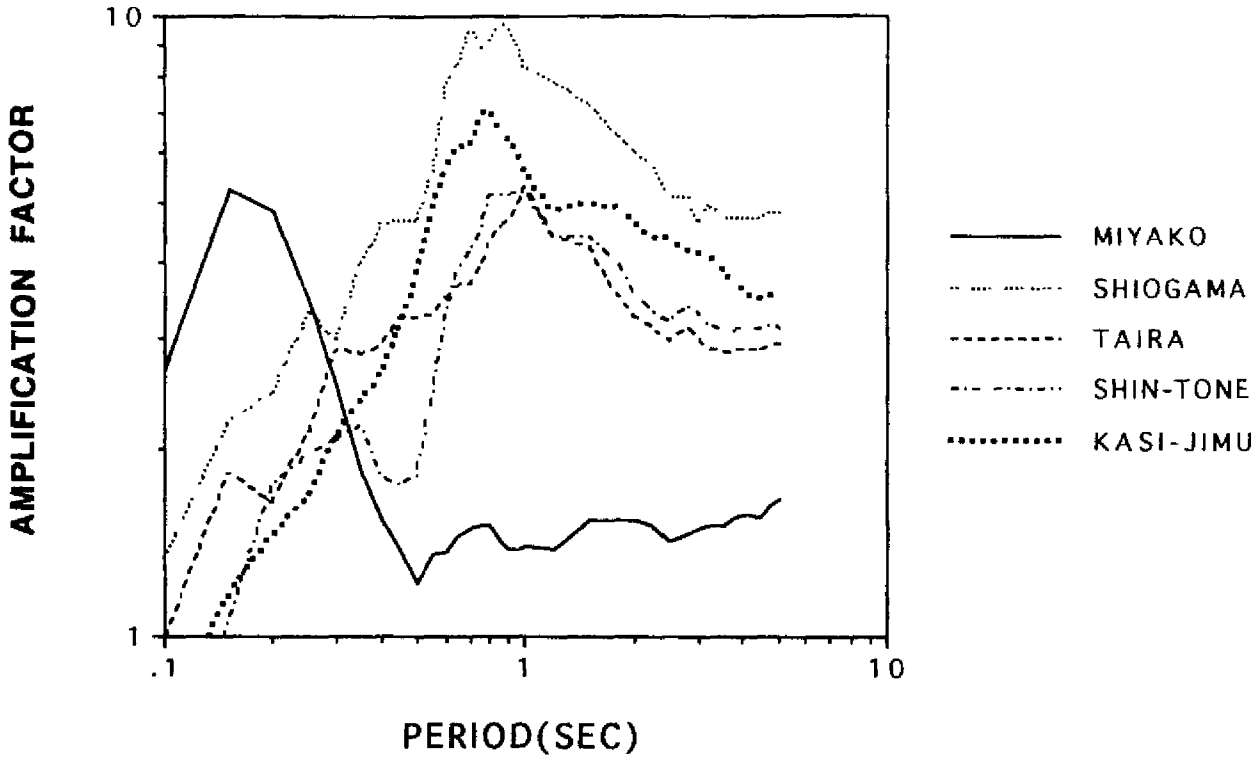

Fig.5-5 **Response Spectra Amplification Factors for 5 Sites(Miyako, Shiogama,Taira, Shintone and Kashima Jimu) in Japan (after Kamiyama and Yanagisawa[9])**

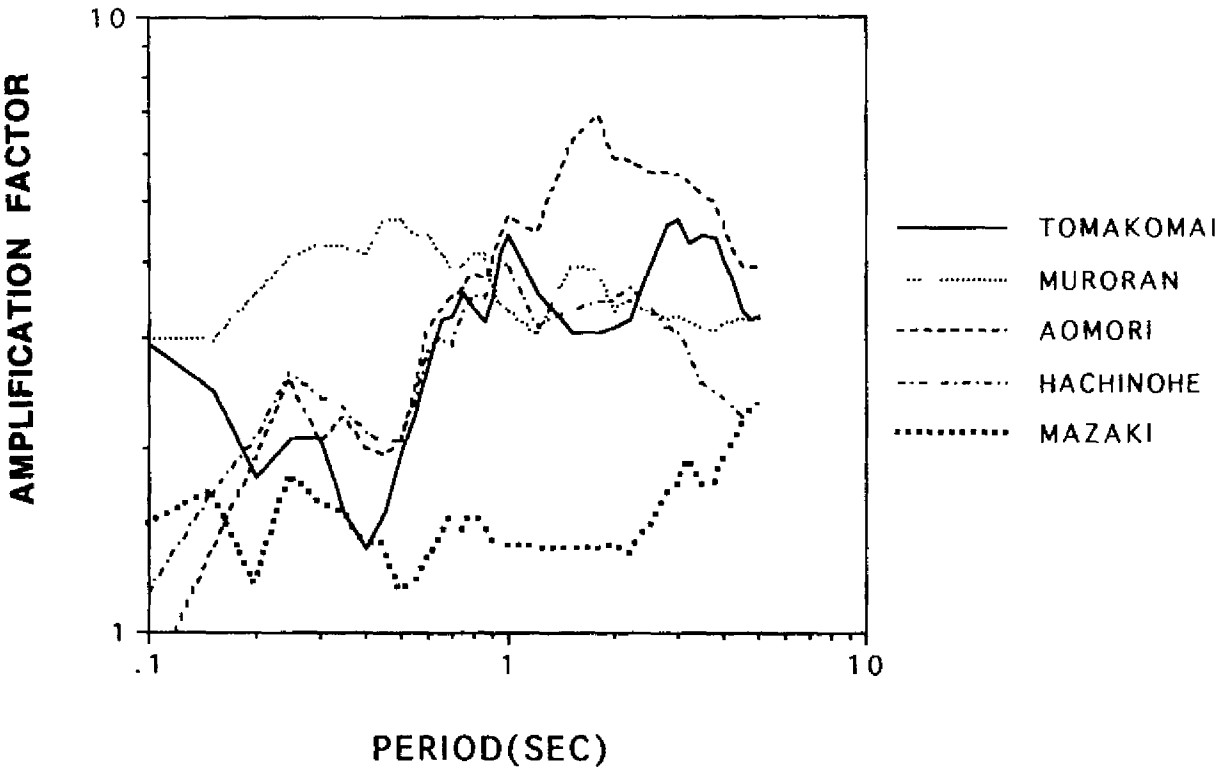

Fig.5-6 Response Spectra Amplification Factors for 5 Sites(Tomakomai, Muroran,Aomori, Hachinohe and Mazaki) in Japan (after Kamiyama and Yanagisawa[9])

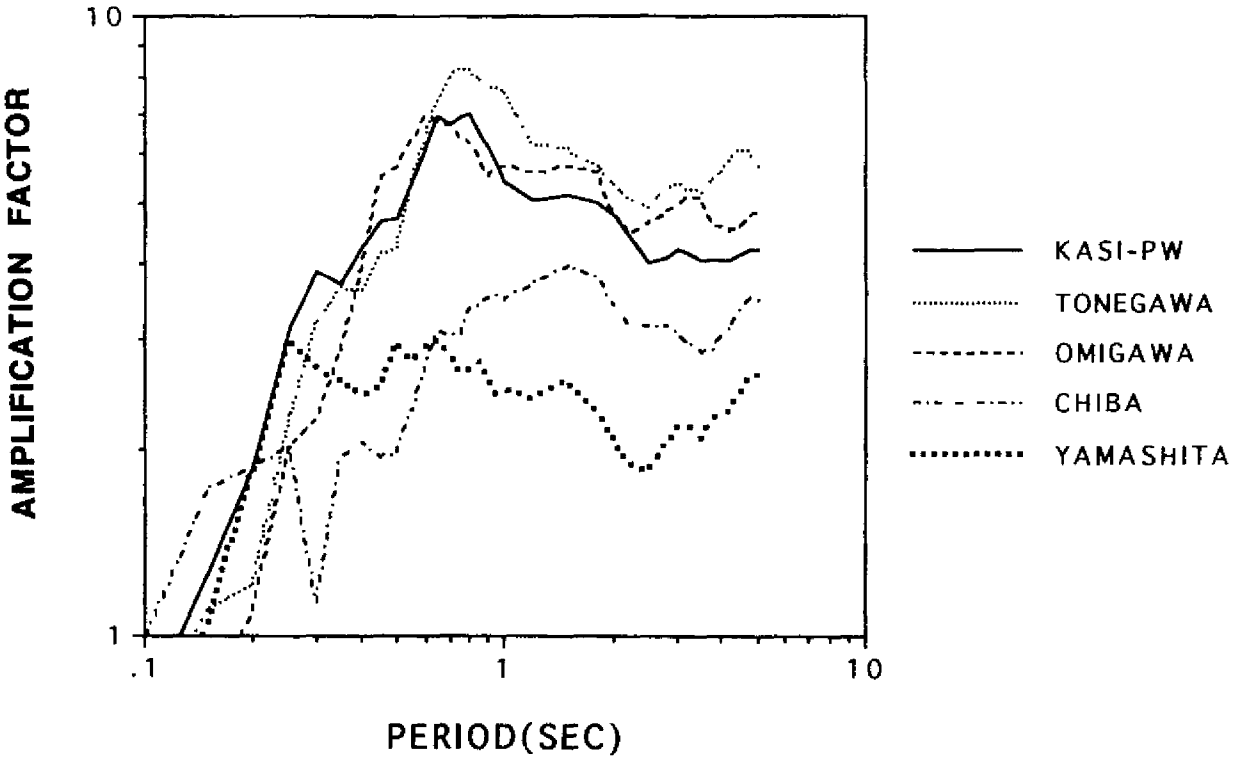

Fig.5-7 Response Spectra Amplification Factors for 5 Sites(Kashima PWR, Tone ESD,Omigawa, Chiba and Yamashita HEN) in Japan (after Kamiyama and Yanagisawa[9])

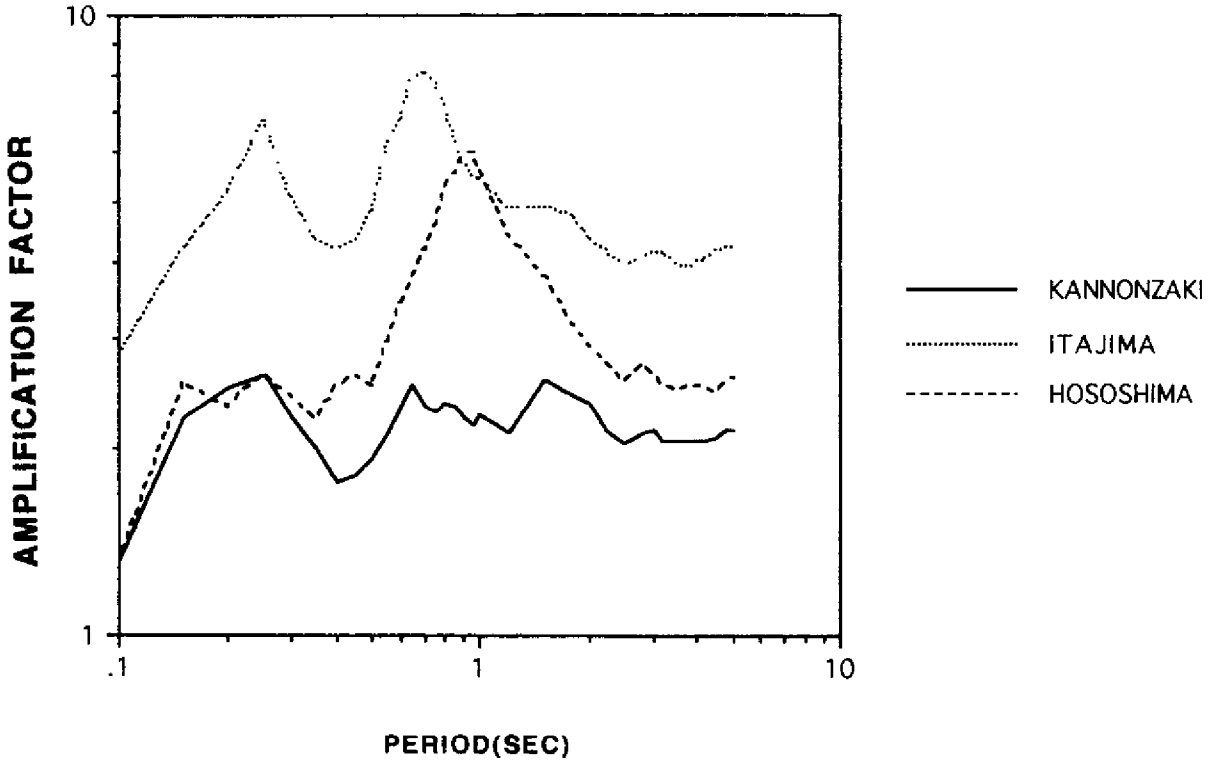

Fig.5-8 Response Spectra Amplification Factors for 3 Sites(Kannonzaki, Itajima and Hososhima) in Japan (after Kamiyama and Yanagisawa[9])

because the peak value results from quite complicated processes. Herein we integrate the amplification spectra in Figs. 5-4 to 5-8 within a period band to investigate how the amplification factors for the peak acceleration, velocity and displacement are associated with their frequency content.

Since short period motions likely control peak acceleration and large period motions likely control peak velocity, band-pass filters were applied to the amplification spectra. The integrated spectral value $\mathbf{SP_i}$ then becomes

$$SP_i = \frac{1}{4.9}\int_{0.1}^{5.0} A_i(T)\,R(T)\,dT \qquad (5.7)$$

where $\mathbf{A_i(T)}$ are the period dependent spectral amplifications shown in Figs. 5-4 to 5-8, $\mathbf{R(T)}$ is a high frequency pass filter for peak acceleration and a low frequency pass filter for peak velocity and T is period.

After a number of trials, the high frequency pass filter in Fig.5-9 was chosen for peak acceleration while the low frequency pass filter in Fig.5-10 was chosen for peak velocity. Figs. 5-11 and 5-12 show the correlations between the amplification factors for peak acceleration and peak velocity at some sites in Table 5-II and their corresponding integrated spectral values by Eq.(5.7). The displacement case is omitted herein because of its close correlation with velocity. We can see from Figs.5-9 through 5-12 that the peak acceleration is determined principally by spectral amplifications in periods leass than about 0.3 sec while the peak velocity is determined by periods greater than about 1.0 sec. This means that local soils respond differently to acceleration and velocity motions with a definite period-dependence. It is clear from this result that a site composed of extremely soft soil with high viscosity is expected to show only small peak acceleration in spite of showing a large peak velocity because such a site has spectral amplification with long-period dominance as well as high attenuation in the short period domain. Consider, for example, the SHIN ISHIKATRI site which will be shown later to consist of a deep layer of relatively soft soils. As shown in Fig.5-4, the spectral amplification at this site is large for periods greater than about 1.0 seconds but comparatively small for periods less than 0.3 seconds. As a consequence the amplification factors for the peak velocity and displacement in Table 5-II are about double the peak acceleration amplification factor. Conversely, a site with a thin superficial layer over hard rock tends to exhibit large peak and small peak, respectively, in acceleration and velocity because of the short-period dominance of its spectral amplification. An example is the Miyako site which

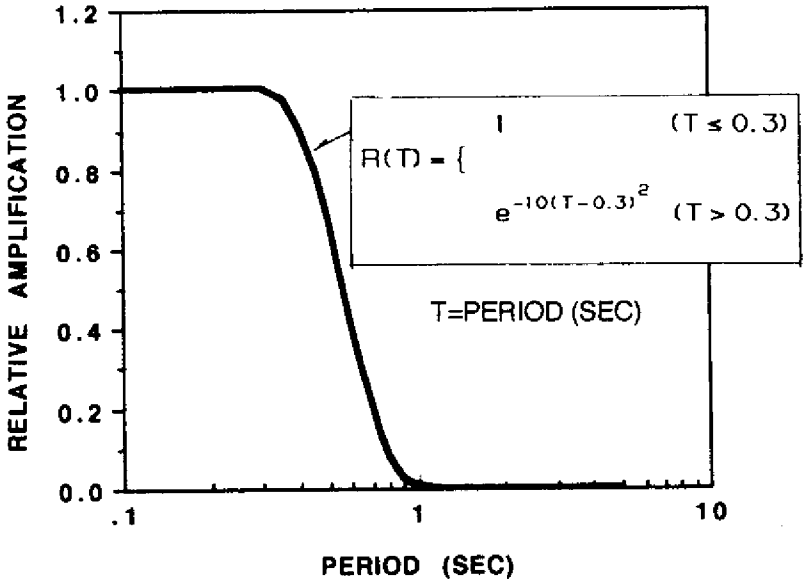

Fig.5-9 High Frequency Pass Filter Applied to Spectra Amplification for Comparison with Peak Acceleration

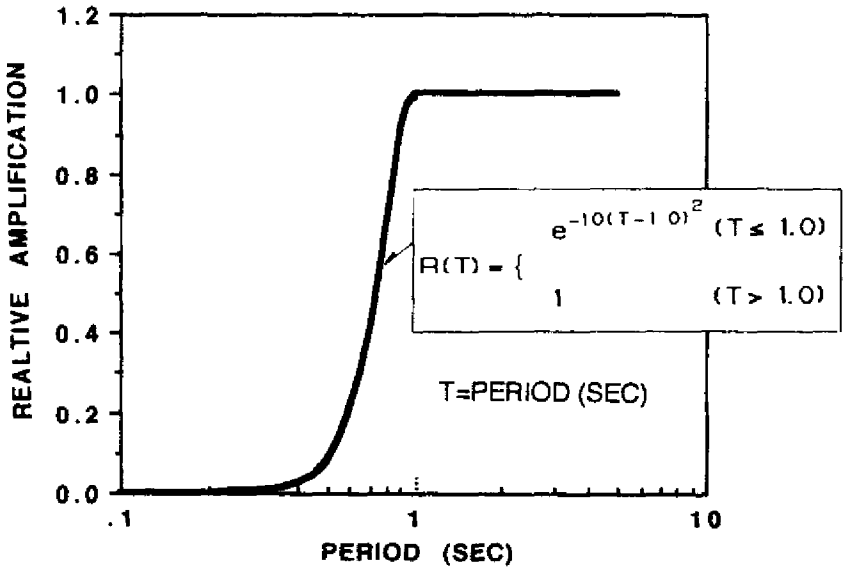

Fig.5-10 Low Frequency Pass Filter Applied to Spectral Amplification for Comparison with Peak Velocity

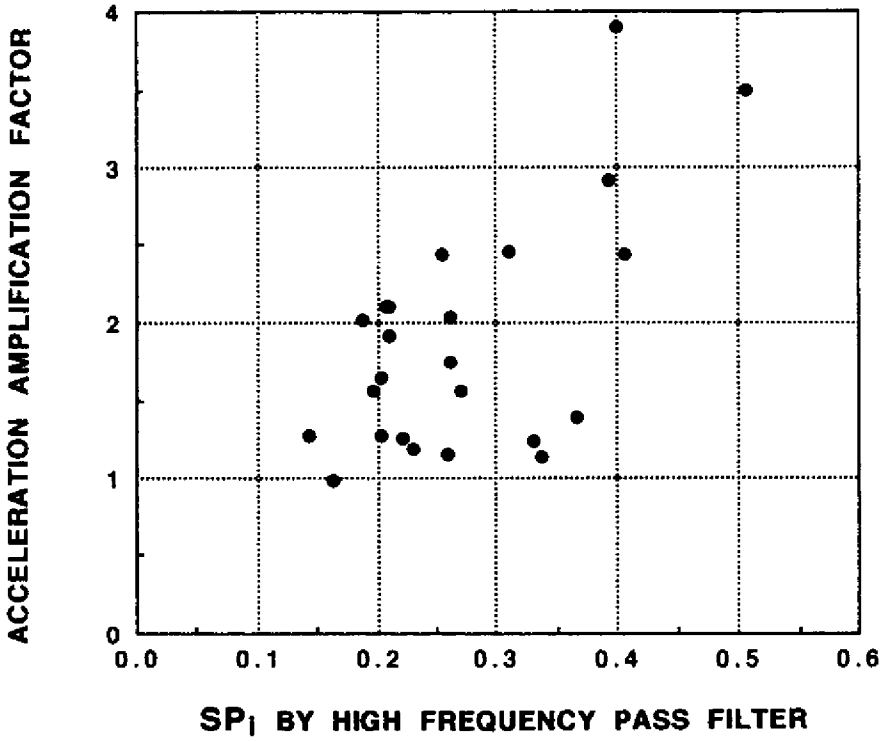

Fig.5-11 Scattergram for Peak Acceleration Amplification Factor and Integrated Spectral Value from Eq.(5.7) Using High Frequency Pass Filter

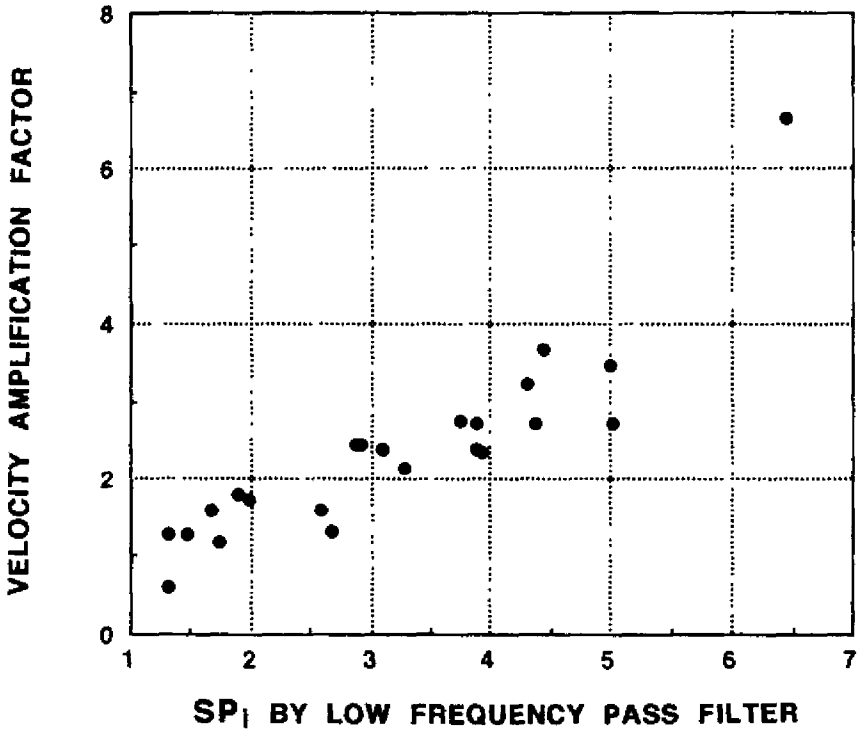

Fig.5-12 Scattergram for Peak Velocity Amplification Factor and Integrated Spectral Value from Eq.(5.7) Using Low Frequency Pass Filter

corresponds to a relatively thin layer over rock. The Miyako site has large spectral amplifications for periods less than 0.3 seconds, as shown in Fig.5-5. The spectral amplification at Miyako is consistent with the small amplification factor for the peak velocity and the relatively large amplification factor for the peak acceleration in Table 5-II.

The above examples suggest that peak velocity can be a candidate parameter more responsible for earthquake damage than peak acceleration which has been regarded as the foremost parameter controlling earthquake damage, because damages were overwhelmingly caused at soft soil sites rather than at firm soil sites in the past earthquakes. In addition, since amplification factors for peak motion are related to different frequency ranges, a two parameter characterization of a site may be appropriate. That is, the seismic hazard for a given site may be given in terms of estimates for both peak acceleration and peak velocity. Peak acceleration would control the design of short period structures while peak velocity would control large period structures.

The difference in the period-dependent amplification between peak acceleration and peak velocity also explains the discrepancy of the reference site noted in the preceding section. The OFUNATO site is not appropriate as a reference site for the peak acceleration while it is justified for peak velocity. Although the OFUNATO site was initially selected as the common reference site because of its outcropping of hard slate, there is a possibility that its surface part has been weathered so as to give a high amplification in short periods. Hence it might fail to offer a proper reference site corresponding to the seismic bed rock for the other sites in the case of the peak acceleration.

5.3 Relation Between the Amplification Factors and the Local Soil Conditions

It is obvious from the foregoing discussion that the peak motion amplification factors are closely related to the corresponding local soil conditions. In order to apply our semi-empirical model to an arbitrary site not included in the present empirical analysis, it is necessary to be able to predict the amplification factors at a site from its local soil conditions. Herein we examine the detailed relation between the empirical amplifications and soil conditions, and propose two methods; one qualitative and the other quantitative for estimating an amplification factor at a new site having soil information.

Soil profiles are available for some of the observation sites in Fig. 3-1. Figs. 5-13(a) to 5-13(q) show the soil profiles at these sites which consist of the soil formation and the standard penetration test results meeting the Japanese Industrial Standard, namely, the N-value. These soil profiles

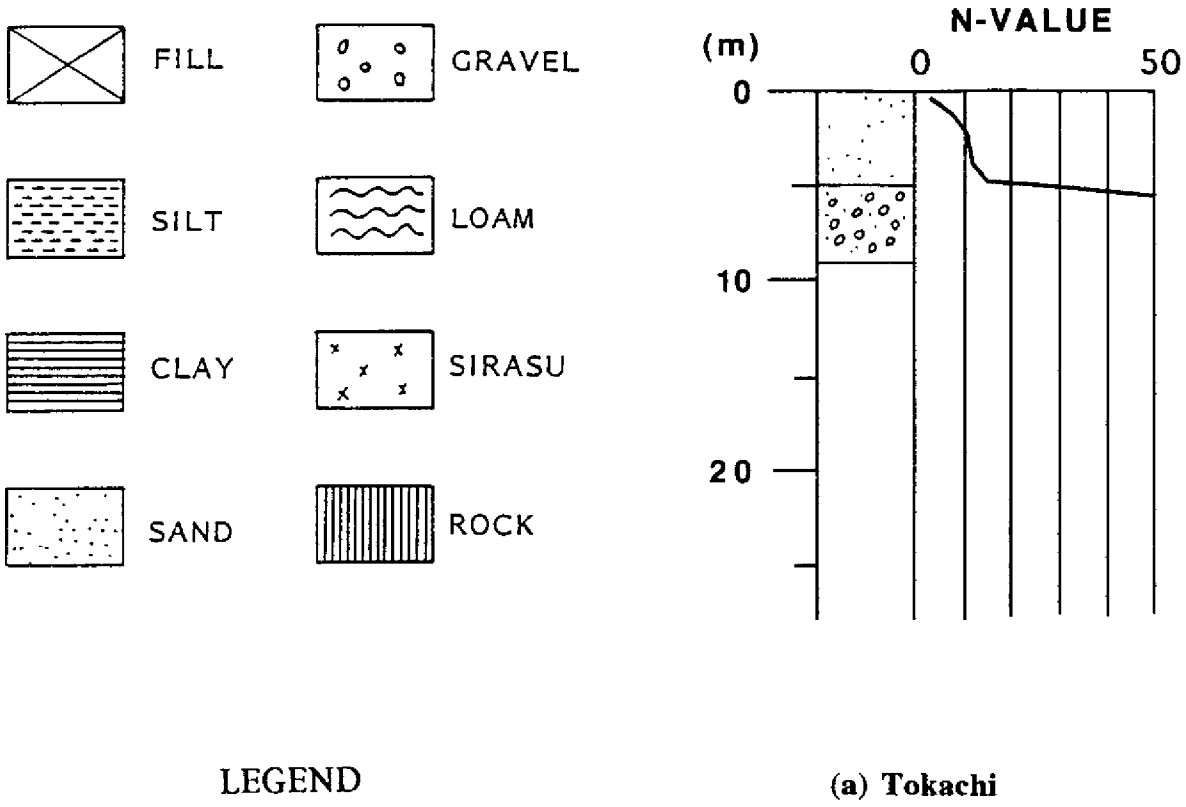

Fig.5-13 Available Soil Profile for Japanese Sites Considered herein

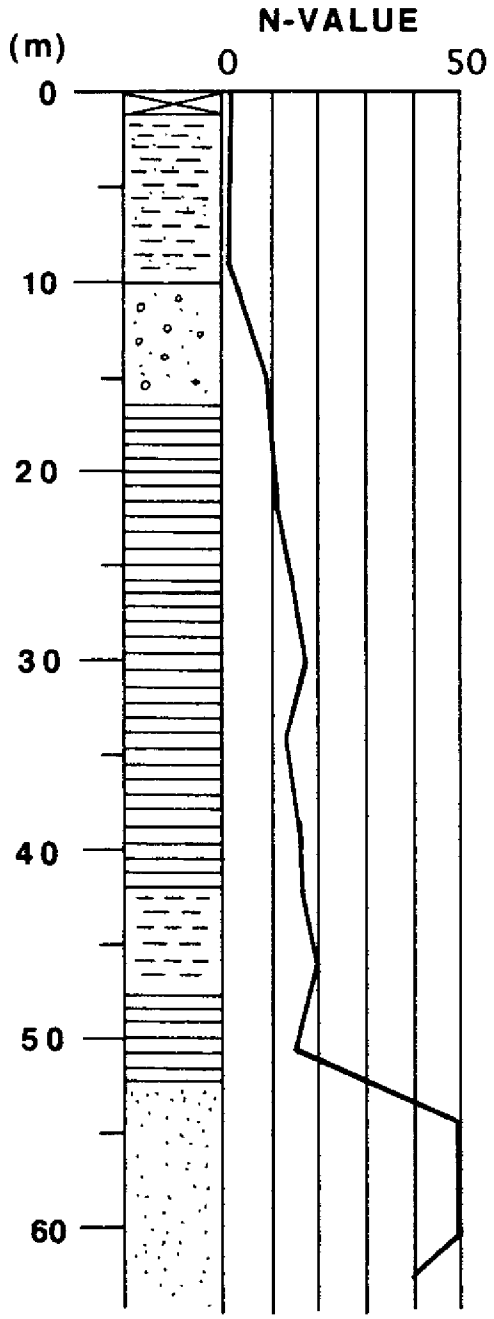

(b) Shin Ishikari

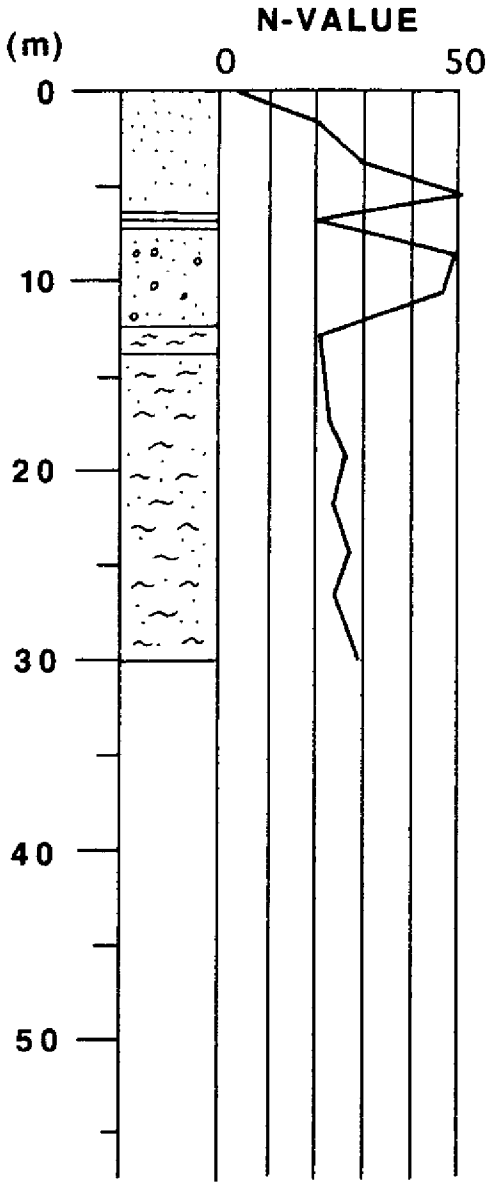

(c) Tomakomai

Fig.5-13 Available Soil Profile for Japanese Sites Considered herein

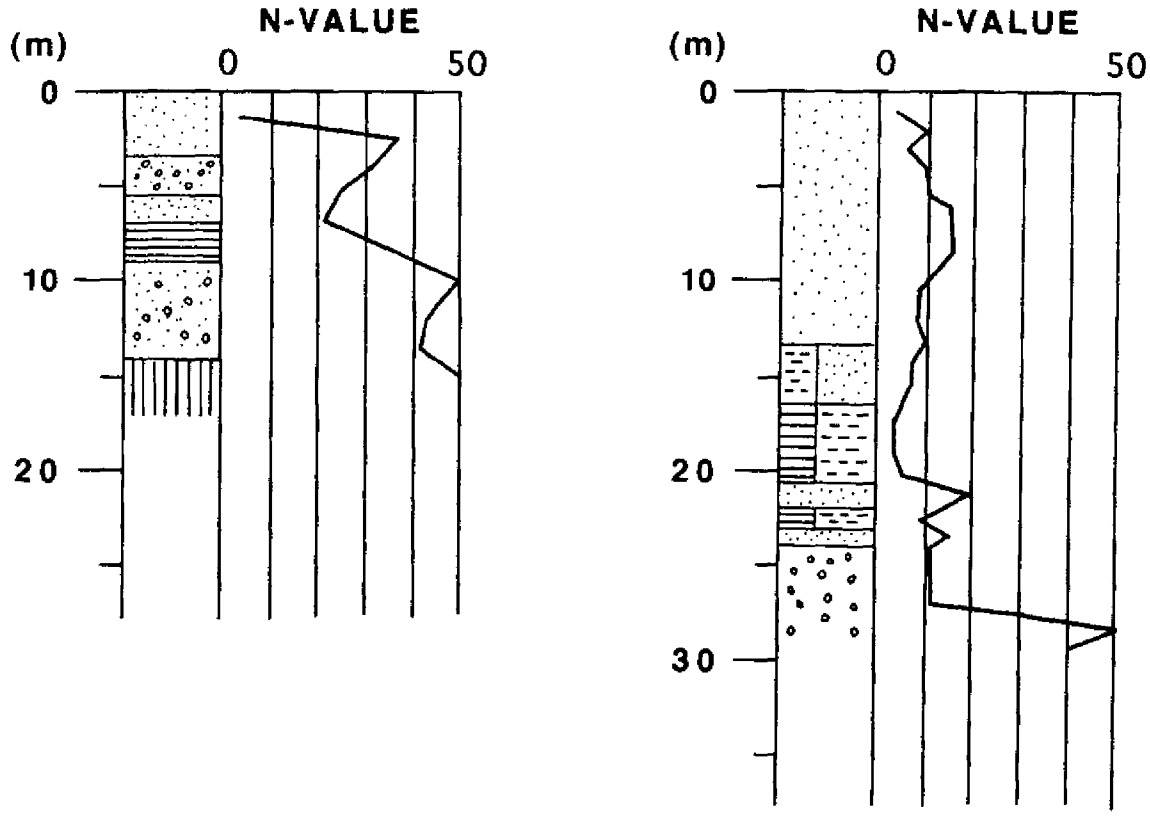

(d) Muroran

(e) Aomori

Fig.5-13 Available Soil Profile for Japanese Sites Considered herein

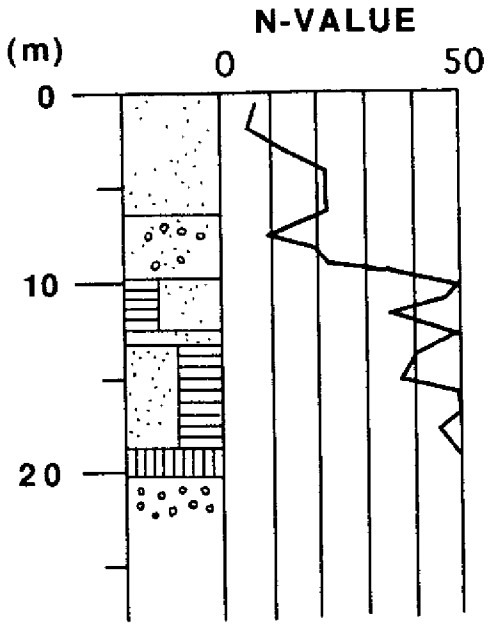

(f) Hachinohe

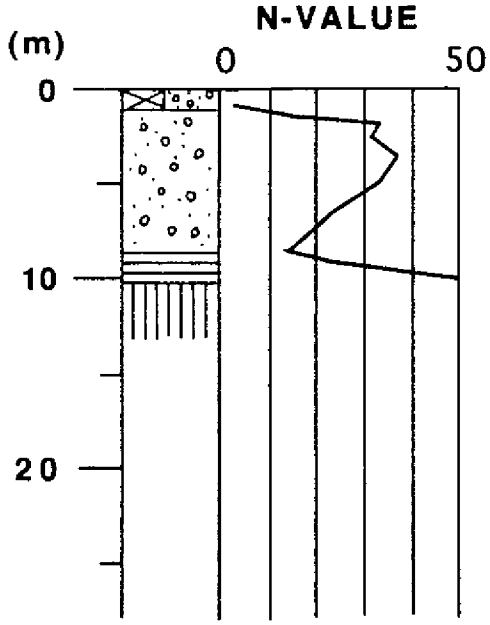

(g) Miyako

Fig.5-13 Available Soil Profile for Japanese Sites Considered herein

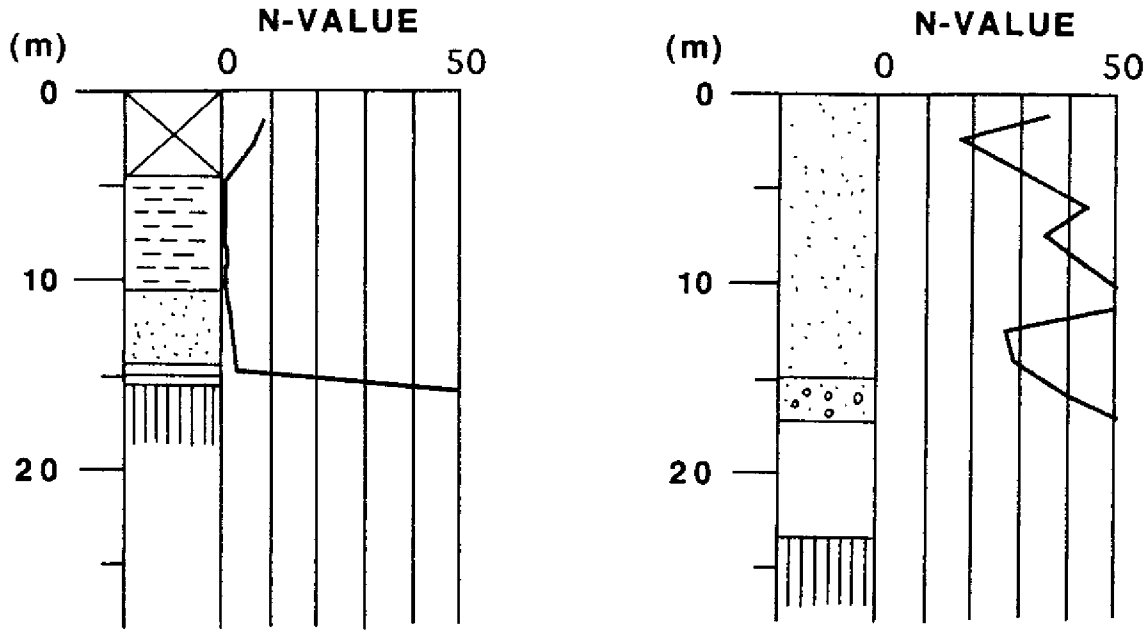

(h) Shiogama

(i) Kashima Jimu

Fig.5-13 Available Soil Profile for Japanese Sites Considered herein

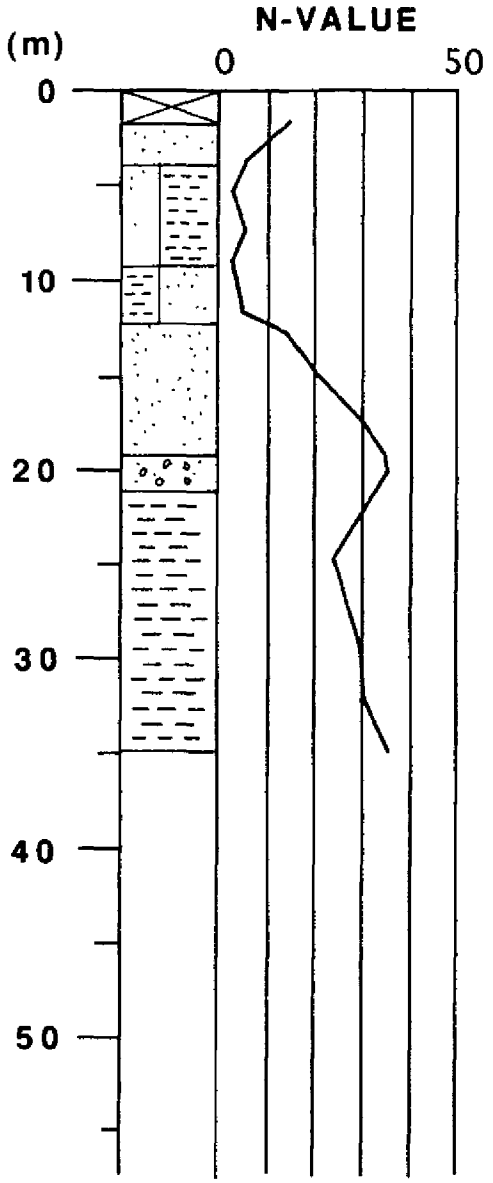

(j) Yamashita Hen

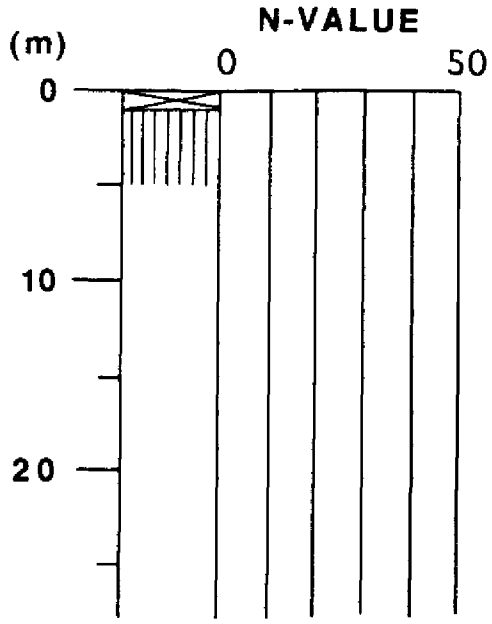

(k) Kannonzaki

Fig.5-13 Available Soil Profile for Japanese Sites Considered herein

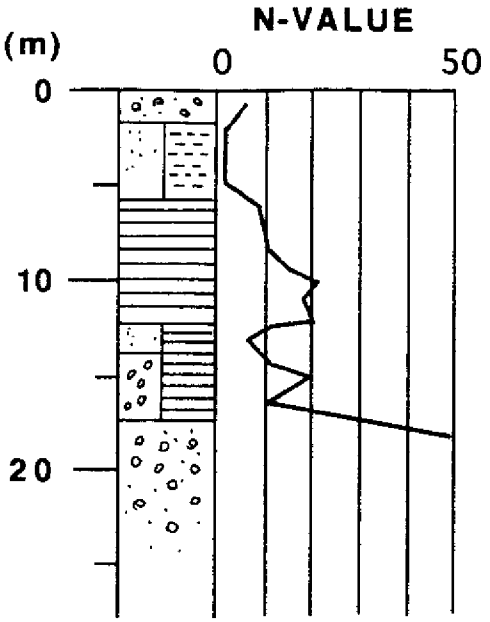

(l) Itajima

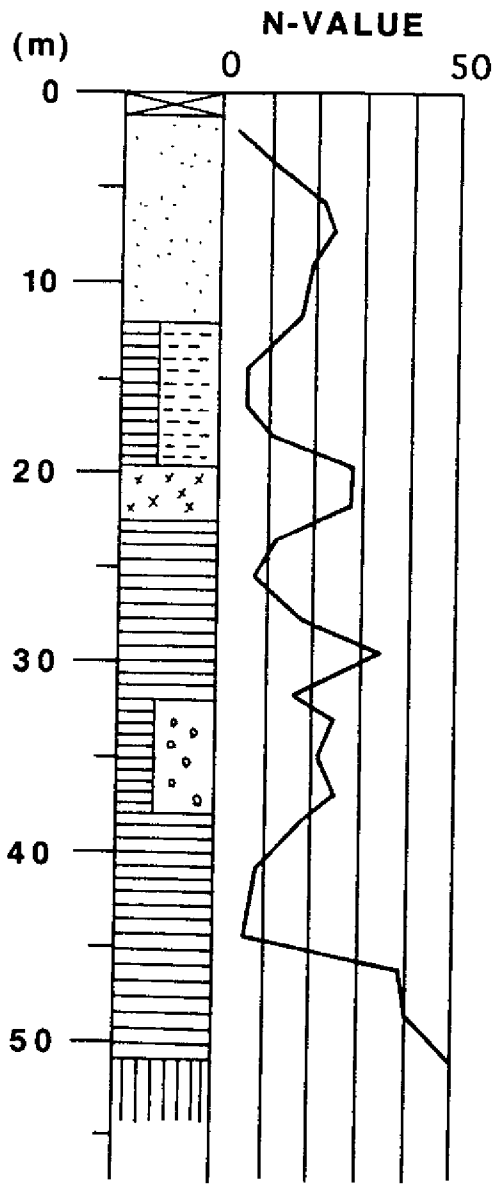

(m) Hososhima

Fig.5-13 Available Soil Profile for Japanese Sites Considered herein

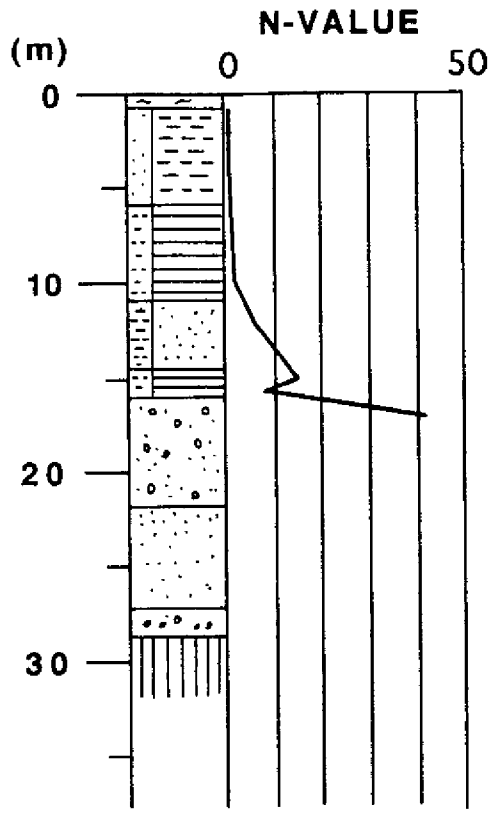

(n) Shinagawa

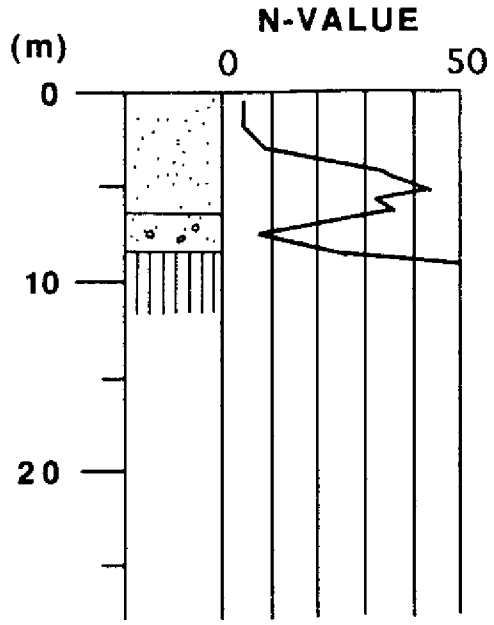

(o) Onahama Ji

Fig.5-13 Available Soil Profile for Japanese Sites Considered herein

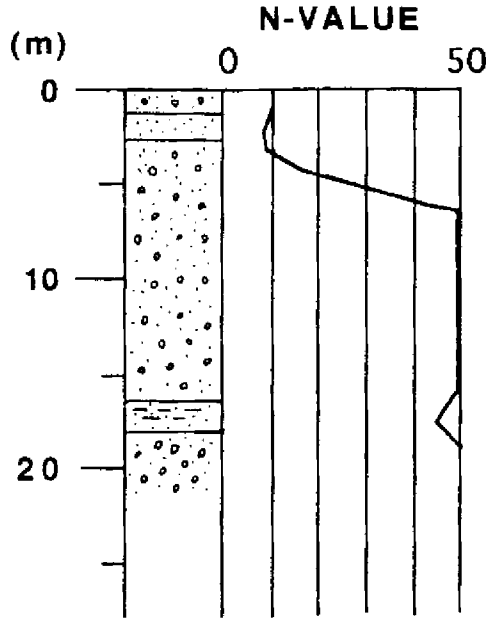

(p) Akita

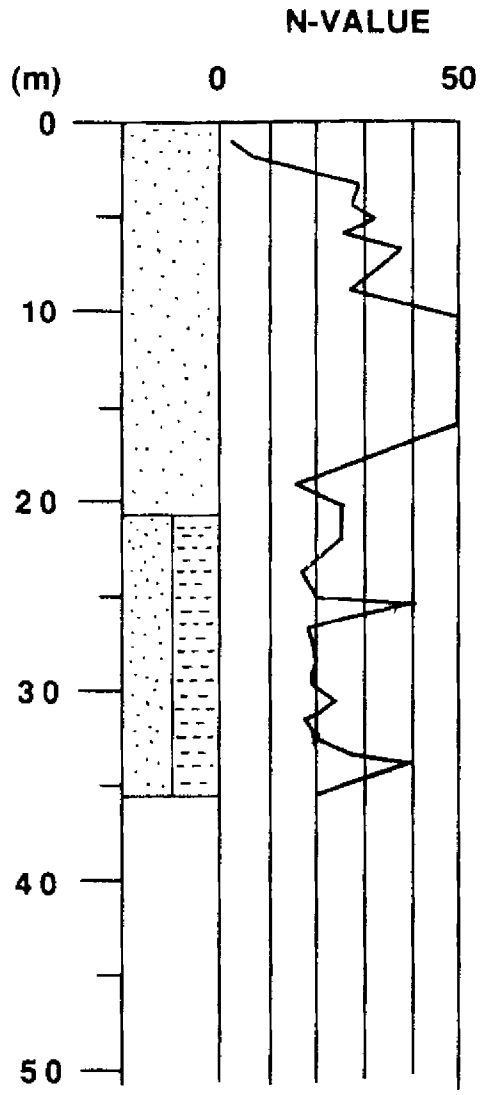

(q) Kashima Zokan

Fig.5-13 Available Soil Profile for Japanese Sites Considered herein

were obtained primarily from the site data compiled by the Port and Harbor Research Institute, Ministry of Transport of Japan[24].

As illustrated in Figs. 5-13(a) to 5-13(q), each observation site has various types of soil formations as well as soil softness. A close look at both Table 5-II and Figs. 5-13(a) to 5-13(q) indicates that the amplification factors vary depending on the formation and the softness of soils. For example, some soft soil sites like SHIN-ISHIKARI, SHIOGAMA, SHINAGAWA etc. represent large amplification factors for peak velocity and displacement while except for SHIN-ISHIKARI they give relatively small amplifications for acceleration. On the other hand, the stiff soil sites such as TOKACHI, MIYAKO etc. show large amplifications in the peak acceleration while they show extremely small amplifications in the peak velocity and displacement. Such a relation between the amplifications and soil profiles suggests a method for estimating the amplification factor at a new site. That is, given a soil profile at a new site, one can approximately predict an amplification factor at the site by looking for a soil profile in Figs. 5-13 (a) to 5-13(q) most similar to the new site profile and selecting its amplification factor. This method is hereafter called the "qualitative method". Since a variety of soil profiles are compiled in Figs. 5-13(a) to 5-13(q), this method may, despite its simplicity, provide an unexpectedly good way for estimating an amplification factor. For example, both SHINAGAWA(Fig.5-13(n) and SHIOGAMA(Fig.5-13(h) have very soft soils($N<10$) for moderate depth(up to about 15 m). The acceleration and velocity amplification factors for these sites in Table 5-II are somewhat similar (2.44 and 3.46 respectively for SHIOGAMA and 1.69 and 2.71 respectively for SHINAGAWA). That is, both these sites have moderate acceleration amplification but significant velocity amplification. Contrast this with TOKACHI(Fig.5-13(a)) and AKITA(Fig.5-13(p)) which have a thin layer (depth of about 5 m) of moderately soft soils($N\sim10$). Both these sites have low to moderate acceleration amplification factors (2.02 and 1.44 respectively) and somewhat similar velocity amplification factors(1.60 and 2.00 respectively).

The quantitative method for a new site is based upon the concept of the vibration impedance ratio. As described previously, the amplification factors for the peak acceleration, velocity and displacement were obtained with respect to the seismic bed rock at our reference site having S wave velocity of 1 to 2 km/sec range. This strictly means that these amplification factors should be related to soil structures overlaying such seismic bed rock. In general, however, seismic bed rock is laid deep and we have almost no opportunity for finding it in a usual soil profile. In addition, one needs elaborate material information of each layer such as P and S waves velocity, Q values, etc. in order to relate soil conditions to the empirical amplification factors. However such material information is available only at some special sites because of the cost. Hence although vibration

impedance and amplification are directly related to P and S wave velocities, density and Q value(damping), herein we use the N-value variation with depth such as shown in Figs.5-13(a) to 5-13(q) which is the typical information available to a designer and is known to have some relation with the rigidity and density of soils.

Furthermore the quantitative method is restricted to peak velocity amplification factors. This is based on two consideration; first of all Table 5-II indicates that the variation in the peak acceleration amplification factors is relatively small and secondly peak velocity is the parameter of interest for lifeline earthquake engineering studies which is the primary purpose of this study. After a number of trials, the following expression C_{amp} was chosen to represent the impedance characteristics and predominant period of a soil profile.

$$C_{amp} = Max\left[\frac{\sqrt{N(x_{i+1})}}{\frac{1}{i}\sum_{j=1}^{i}\sqrt{N(x_j)}}\right] \times \frac{x_M}{\frac{1}{M}\sum_{j=1}^{M}\sqrt{N(x_j)}} \qquad (5.8)$$

where $\mathbf{x_j}$ is the depth of the **j-th** N-value, $\mathbf{N(x_j)}$ is the N-value corresponding to the depth of $\mathbf{x_j}$, **i** is the order number of N-value (i=1~L-1), L is the total number of N-values and M is the the order number maximizing the first term on the right-hand side.

In Eq.(5.8), the first term on the right-hand side is the maximum value of the expression within the parenthesis for **i=1** to **i=L-1**, and **M** is the value **i** which maximizes the expression. Eq.(5.8) was derived as a simple approximation based on the concept of the maximum vibrational impedance ratio and the corresponding predominant period. A caluculation of C_{amp} is shown in Appendix B. C_{amp} was estimated for each soil profile in Figs. 5-13(a) to 5-13(q) and is plotted against the corresponding the peak velocity amplification factor $\mathbf{AMP_i}$ **(v)**, in Fig.5-14. Though there is some variance, a positive relation is seen between $\mathbf{c_{amp}}$ and $\mathbf{AMP_i(v)}$. A linear regression expression for $\mathbf{AMP_i(v)}$ as a function of $\mathbf{c_{amp}}$ is

$$AMP_i(v) = 1.25 + 0.112\, C_{amp} \qquad (5.9)$$

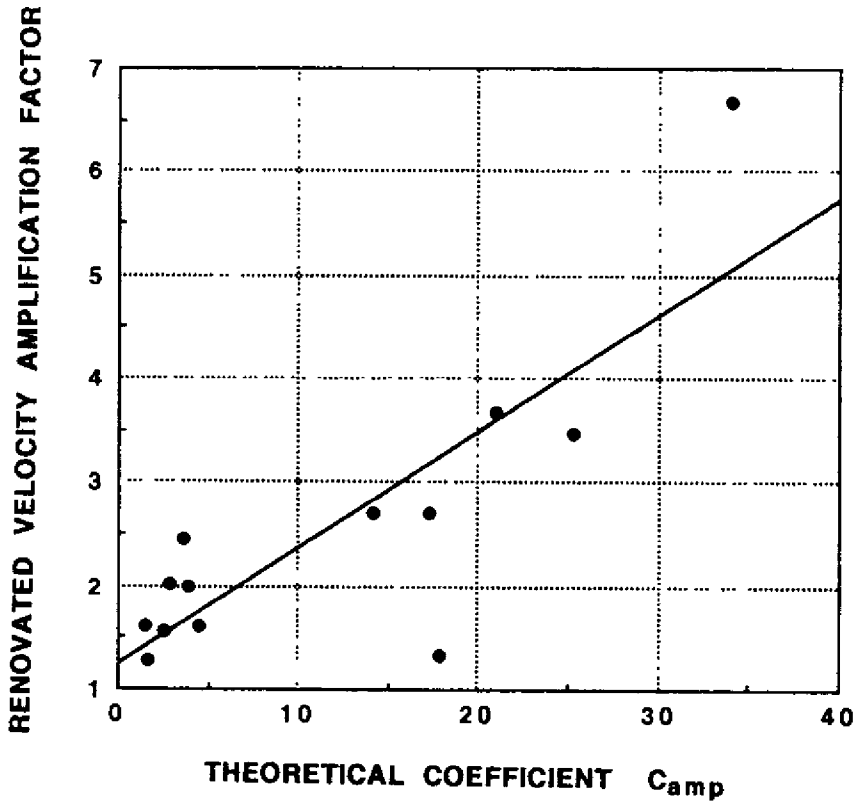

Fig.5-14 Scattergram of Velocity Amplification Factor and Coefficient C_{amp}

Although Eq.(5.8) is simplified and typically would not incorporate information on deep structure down to the seismic bed rock nor Q values, it yields reasonable estimates of the amplification factor for peak velocity. The equation will be applied in a later section.